HSP90 empowers evolution of resistance to hormonal therapy in human breast cancer models

Luke Whitesell[a,1], Sandro Santagata[a,b], Marc L. Mendillo[a], Nancy U. Lin[c], David A. Proia[d], and Susan Lindquist[a,e,f,1]

[a]Whitehead Institute for Biomedical Research, Cambridge, MA 02142; [b]Department of Pathology, Brigham and Women's Hospital and Harvard Medical School, Boston, MA 02115; [c]Department of Medical Oncology, Dana–Farber Cancer Institute, Boston, MA 02215; [d]Synta Pharmaceuticals, Lexington, MA 02421; [e]Department of Biology, Massachusetts Institute of Technology, Cambridge, MA 02142; and [f]Howard Hughes Medical Institute, Cambridge, MA 02142

The efficacy of hormonal therapies for advanced estrogen receptor-positive breast cancers is limited by the nearly inevitable development of acquired resistance. Efforts to block the emergence of resistance have met with limited success, largely because the mechanisms underlying it are so varied and complex. Here, we investigate a new strategy aimed at the very processes by which cancers evolve resistance. From yeast to vertebrates, heat shock protein 90 (HSP90) plays a unique role among molecular chaperones by promoting the evolution of heritable new traits. It does so by regulating the folding of a diverse portfolio of metastable client proteins, many of which mediate adaptive responses that allow organisms to adapt and thrive in the face of diverse challenges, including those posed by drugs. Guided by our previous work in pathogenic fungi, in which very modest HSP90 inhibition impairs resistance to mechanistically diverse antifungals, we examined the effect of similarly modest HSP90 inhibition on the emergence of resistance to antiestrogens in breast cancer models. Even though this degree of inhibition fell below the threshold for proteotoxic activation of the heat-shock response and had no overt anticancer activity on its own, it dramatically impaired the emergence of resistance to hormone antagonists both in cell culture and in mice. Our findings strongly support the clinical testing of combined hormone antagonist-low-level HSP90 inhibitor regimens in the treatment of metastatic estrogen receptor-positive breast cancer. At a broader level, they also provide promising proof of principle for a generalizable strategy to combat the pervasive problem of rapidly emerging resistance to molecularly targeted therapeutics.

estrogen receptor | antiestrogen | drug resistance | tumor progression | tamoxifen

Drastically limiting the efficacy of targeted therapeutics, the emergence of drug resistance in advanced cancers remains nearly inevitable. From yeast to vertebrates, the molecular chaperone heat shock protein 90 (HSP90) allows organisms to adapt and thrive in the face of diverse challenges, including those posed by drugs and environmental stressors (1, 2). It does so by regulating the folding of a highly diverse portfolio of metastable client proteins, many mediating adaptive responses (3, 4).

However, this role for HSP90 in adaptation is greatly magnified by its ability to promote the evolution of heritable new traits. To buffer the proteome against unexpected environmental challenges, HSP90 is present in large excess under normal circumstances. This buffering capacity allows it to modulate the manifestation of preexisting and newly acquired genetic variation within heterogeneous populations of cells, and even whole organisms, thereby dramatically expanding the range of phenotypes on which selection can act (1, 2, 5–7). As a dramatic, therapeutically relevant example, we have shown that this HSP90 buffer enables fungal pathogens spanning ~1 billion years of evolution to evolve and maintain resistance to every major antifungal in general use (8, 9). Now we ask whether HSP90 might serve a similar role in buffering the molecular and genetic heterogeneity present in human tumors and whether low-level inhibition might limit the emergence of drug resistance.

At this time, HSP90 inhibitors are being developed as anticancer therapeutics, with a much simpler rationale: Many proteins that drive the malignant phenotype depend on HSP90's protein-folding activities for their function (10–13). The hope is that the "addiction" of cancer cells to such client proteins will create a therapeutic window: Substantial HSP90 inhibition would block the maturation of oncogenic "drivers" without harming normal cells. The rub is that an important normal function of HSP90 is to bind the stress-responsive transcription factor heat-shock factor 1 (HSF1) and repress its activities. High levels of HSP90 inhibition, therefore, activate HSF1, which has recently emerged as a powerful enabler of malignancy in both cancer cells and the stromal cells that support them (14, 15).

Ironically, the biomarker that has been most broadly used in clinical trials to verify that high, oncoprotein-depleting levels of HSP90 inhibition have been achieved is the increased expression of HSP70. Because HSP70 expression is regulated by HSF1, it serves as a surrogate marker for the activation of this factor (16, 17). Thus, in practice, at the levels of HSP90 inhibition currently sought in the clinic, the very real benefits that might be achieved through the differential vulnerability of cancer cells are likely to be attenuated by the activation of HSF1.

Here we ask whether HSP90 could be effective against cancers in an entirely different manner. Our previous work has demonstrated an ancient, highly conserved function for HSP90 in supporting the evolution of new traits in diverse organisms. Might the emergence of resistance to an anticancer therapeutic in the heterogeneous population of cells that make up a cancer

---

Significance

Although hormonal therapies for estrogen receptor-positive (ER+) breast cancer make up the earliest, and arguably most effective, "molecularly targeted" anticancer drugs, continued progress in controlling metastatic disease has been slow. Heterogeneity and the complexity of signaling in advanced cancers have frustrated efforts to prevent the rapid evolution of resistance to hormonal therapies, as well as kinase inhibitors and other agents. On the basis of earlier work defining the role of heat shock protein 90 (HSP90) in other evolutionary processes, we tested whether low-level HSP90 inhibition would limit the evolution of hormone resistance in breast cancer models. Results in culture and in mice provide support for a readily implemented strategy by which the heterogeneity and evolvability of metastatic ER+ breast tumors, and perhaps other advanced cancers, might be controlled.

MEDICAL SCIENCES

be prevented by modest, non-HSF1-activating levels of HSP90 inhibition (16–18)? As a specific test of this hypothesis, we examined whether levels of HSP90 inhibition that are much lower than those commonly used could restrict the ability of tumors to evolve resistance to hormonal therapy in models of estrogen receptor-positive (ER+) breast cancer. Almost all women with advanced ER+ breast cancer inexorably progress through multiple forms of hormonal therapy, to ultimately die of multidrug-resistant disease (18, 19). If low levels of HSP90 inhibition have the power to stop this evolutionary process, it could both address an urgent unmet need and provide compelling support for the broader therapeutic potential of targeting evolutionary mechanisms (20–22).

Results

Modest HSP90 Inhibition Limits Tam Resistance in Culture. We first defined threshold exposure conditions for an HSP90 inhibitor that alone would exert no direct effect on growth of the ER+ breast cancer cell line MCF-7. This line was established from the pleural effusion of a patient with metastatic disease and displays considerable clonal heterogeneity at the genetic and phenotypic levels (23). As the HSP90 inhibitor, we chose ganetespib, a synthetic second-generation agent in late-stage clinical development that has markedly improved pharmacology over earlier natural product-derived compounds (24, 25). We found that concentrations of ganetespib ≤10 nM met the specified criterion for lack of growth inhibition (Fig. 1A). We then examined clonogenic outgrowth of cells cultured continuously for 1 mo in tamoxifen (4-hydroxytamoxifen, Tam) a widely used antiestrogen. Low nanomolar concentrations of ganetespib, which alone did not alter cell accumulation, markedly reduced the appearance of Tam-resistant clones (Fig. 1B and Fig. S1A). This effect was not restricted to HSP90 inhibition by ganetespib because an alternate chemotype, the prototypical natural product HSP90 inhibitor geldanamycin, also dramatically suppressed the emergence of Tam-resistant clones at concentrations that did not alter cell accumulation on their own (Fig. S1B).

The powerful effect of modest HSP90 inhibition was confirmed genetically, using low-level, stable knockdown of either *HSP90α* or *HSP90β* in MCF-7 cells (Fig. S2 *A and B*). Knockdown of either isoform had no general effect on growth in the absence of Tam, but it dramatically reduced the emergence of Tam-resistant clones during long-term culture.

To determine whether this modest level of knockdown did actually affect the HSP90 buffer, we examined the maturation of two well-established HSP90 client proteins, the receptor tyrosine kinases insulin-like growth factor 1 receptor (IGF-1R) and human epidermal growth factor receptor 2 (HER2). Under basal conditions, flow cytometry demonstrated no differences in receptor levels. However, the hairpins did reduce available HSP90 capacity because on challenge with geldanamycin, surface expression of these kinases was more severely affected in cells carrying the knockdown hairpins (Fig. S2C).

One explanation for the effect of HSP90 inhibitor on the emergence of Tam resistance is classical drug–drug synergy. This common effect increases anticancer activity by altering the dose–response relationship for one agent in the presence of another (26). To test for pharmacologic synergy, we measured the concentration-dependent inhibition of MCF-7 cell accumulation after 5 d in various concentrations of ganetespib and the same saturating concentration of Tam (1 μM) used in clonogenic assays. Across a broad range of ganetespib concentrations, we saw no synergistic interaction with Tam in short-term growth assays (Fig. 1A). Specifically, at the concentrations used in our clonogenic assays, ganetespib with Tam had no greater effect than Tam alone (Fig. 1A, inset).

Combination Treatment Limits Escape from Cell Cycle Arrest. We treated MCF-7 cells under the same conditions used for clonogenic assays, but for only 10 d. Vehicle control and ganetespib-
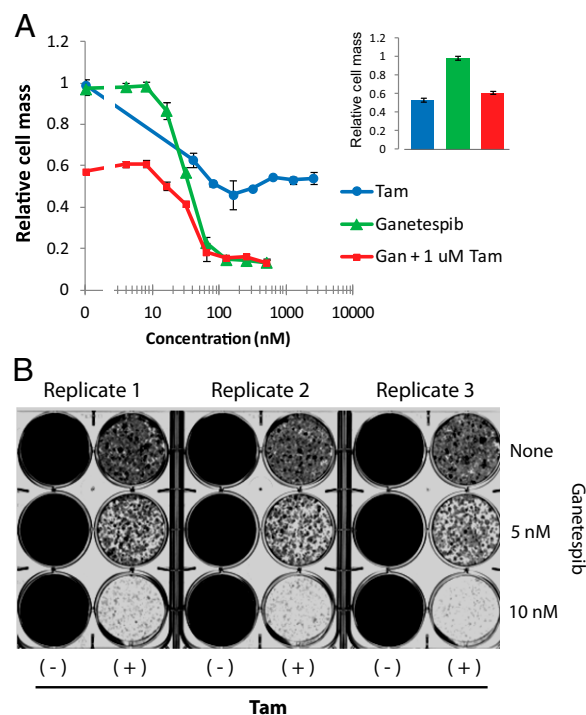

Fig. 1. Very modest pharmacologic inhibition of HSP90 function limits the emergence of Tam resistance in cell culture. (*A*) Dose–response testing. MCF-7 cells were cultured for 5 d with ganetespib (Gan), Tam, or a combination of Tam (1 μM) plus serial dilutions of Gan. Concentration-dependent inhibition of relative MCF-7 cell mass was measured by standard sulforhodamine B protein assay. (*B*) Clonogenic assays. MCF-7 cells were cultured continuously in the presence of the indicated concentrations of the HSP90 inhibitor, ganetespib, with or without concurrent Tam (1 μM). After 1 mo, cells were fixed with cold methanol, and the macroscopic outgrowth of resistant colonies was visualized by staining with Diff-Quik. Photomicrographs of representative wells are provided in Fig. S1A.

treated cultures became densely confluent. In cultures exposed to Tam alone, emergent foci of resistant cells had begun to appear on a background monolayer of growth-inhibited cells. In cultures treated with a combination of Tam and ganetespib, the monolayer was still largely intact, but no such foci were apparent (Fig. 2A). We then measured relative mRNA levels genome-wide. In contrast to typical high-level HSP90 inhibition, the low concentration of ganetespib used in our experiments induced changes in the expression of only a small number of genes. Importantly, stress response and heat-shock protein genes were notably absent, indicating that HSF1 had not been activated (Fig. 2B, Fig. S3A, and Dataset S1). Likewise, low-level HSP90 inhibition did not appear to directly impair the transcriptional activating activity of the ER, a well-recognized client protein. Ganetespib-only treatment had no consistent effect on the expression of genes that had consensus estrogen response elements within 2 kb of their transcriptional start sites and that were downregulated ≥twofold by treatment with Tam alone (Fig. S3B).

As expected from its known cytostatic activity, with Tam treatment, changes in cell cycle-associated genes were seen. Combination Tam and ganetespib treatment, however, greatly accentuated the drop in cell cycle-associated gene expression and expanded the number of genes with reduced expression in the categories of "cell cycle" and "DNA replication" (Fig. 2B). Strikingly, combination treatment also augmented the downregulation of genes with regulatory motifs bound by E2F family transcription factors. E2F regulates progression through several points in the cell cycle, especially the G1-S transition, and has
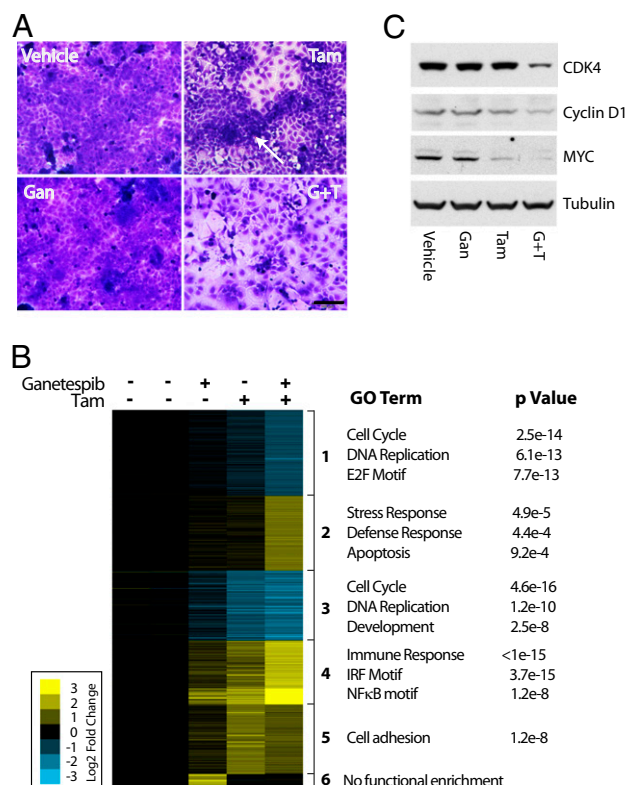
Fig. 2. More uniform and profound cell cycle arrest is caused by exposure to a combination of Tam and low-dose HSP90 inhibitor than to either agent alone. (A) Photomicrographs of Diff-Quick-stained MCF-7 cell monolayers after 10 d in culture with Vehicle (DMSO 0.1% vol/vol and ethanol 0.01% vol/vol), Tam 1 μM, Gan 10 nM, or Gan +Tam (G+T, 1 μM + 10 nM). The white arrow indicates outgrowth of a Tam-resistant focus. All images were obtained at the same magnification. (Scale bar, 50 μm.) (B) Relative mRNA expression levels and gene set enrichment analysis for cells treated as in A. (C) Immunoblotting to assess levels of the indicated proliferation-associated proteins in lysates prepared from cultures treated as in A. Tubulin is used as a loading control.

been implicated in resistance to hormone deprivation (27, 28). Increased expression of genes associated with both stress responses and apoptosis was another unique feature of the transcriptional profile induced by combination treatment (Fig. 2B). In agreement with our transcriptional profiling, low-dose ganetespib alone did not affect the levels of several cell cycle progression-associated proteins, and the effect of Tam alone was mixed (Fig. 2C). When ganetespib was combined with Tam, however, cyclin-dependent kinase 4 (CDK4), Cyclin D1, and myelocytomatosis (MYC) levels were all strongly and uniformly reduced, indicating a more complete, homogeneous treatment response.

Effect of Modest HSP90 Inhibition on Hormone Resistance Is Not Limited to Tam. To test the generality of our findings, we next asked whether low-level HSP90 inhibition would also block the emergence of resistance to fulvestrant (Fulv), a mechanistically distinct hormone antagonist. In contrast to Tam, which drives association of the ER with DNA in repressive transcriptional complexes, the pure antiestrogen Fulv induces proteasome-mediated degradation of the ER (29). In clonogenic assays, combination ganetespib–Fulv treatment profoundly inhibited the emergence of Fulv resistance in MCF-7 cells. Again, this occurred at concentrations of ganetespib that alone had no effect on cell cycle progression (Fig. 2 B and C) or cell accumulation over the course of month-long assays (Fig. 3A). Furthermore, the effect was not restricted to MCF-7 cells. Ganetespib–Fulv combination treatment was also effective against the established ER+

lines T47D (Fig. 3A) and ZRF-75.1 (Fig. S4). Demonstrating the specificity of these effects, combination treatment had no effect on the ER-negative breast cancer line HCC-38.

Because expression profiling had revealed a striking downregulation of genes controlled by the E2F family of transcription factors, we engineered our breast cancer lines to express luciferase under the control of E2F response elements. After 5 d, before cytological changes were evident, Fulv reduced E2F reporter activity in the ER+ cell lines (Fig. 3B). As expected for an ER-negative line, Fulv did not affect reporter activity in HCC-38 cells, either alone or in combination with ganetespib. In ER+ cells, however, low-level ganetespib induced a more profound decline in reporter activity than was achievable by Fulv alone.

Impairment of Multiple Bypass Mechanisms Helps Limit Resistance. To begin investigating mechanisms by which the addition of low-level HSP90 inhibition could prevent the emergence of resistance, we assayed MCF-7 lysates for the levels of key proteins in pathways previously implicated in the development of hormone resistance. As expected, Tam mildly increased ER levels because it does not destabilize the ER but, instead, prolongs its association with DNA in repressive transcriptional complexes (29) (Fig. S5A). In contrast, Fulv reduced ER levels, as expected. Low-dose ganetespib did not reduce ER levels but did block the
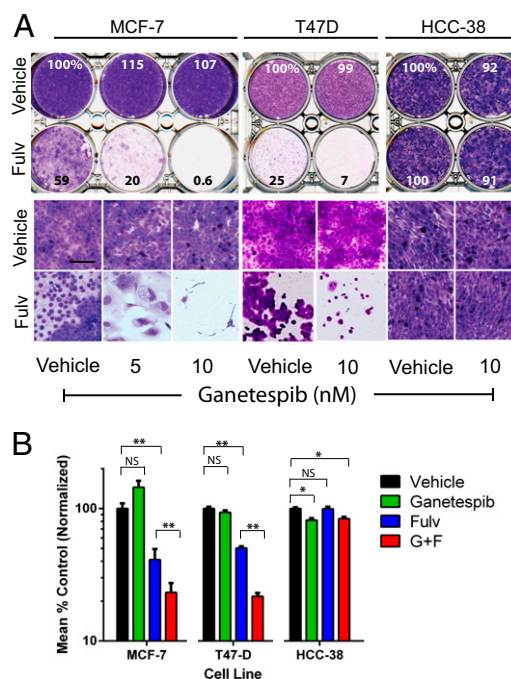

Fig. 3. Very modest pharmacologic inhibition of HSP90 limits the emergence of Fulv resistance in ER+ breast cancer cells. (A, Upper) Macroscopic images of Diff-Quick-stained wells after culture for 1 mo in the indicated concentrations of ganetespib, with or without concomitant Fulv (1 μM). (Inset) Relative cell number per well, expressed as percentage vehicle control, was monitored using Sytox green fluorescence as a measure of DNA content. MCF-7 and T47D are estrogen-responsive human breast cancer cell lines; HCC-38 is a triple-negative, estrogen-independent cell line. (Lower) Photomicrographs obtained from the same wells. All images were acquired at the same magnification. (Scale bar, 50 μm.) (B) Combined treatment enhances the inhibition of E2F transcriptional activating activity. The indicated cell lines were stably transduced with an E2F-regulated luciferase reporter construct and treated as indicated for 10 d: vehicle (0.1% DMSO + 0.01% ethanol), ganetespib (10 nM), Fulv (1 μM), and G+F (ganetespib 10 nM + Fulv 1 μM). Reporter activity is normalized to the protein concentration in each lysate. Mean of quadruplicate determinations is presented. Error bars, SEM; *$P < 10^{-2}$, **$P < 10^{-3}$ (Student t test, two-sided, unpaired).

MEDICAL SCIENCES

increase induced by Tam. More striking, it also enhanced ER depletion by Fulv. We also looked at compensatory up-regulation of receptor tyrosine kinase signaling. Such up-regulation, especially of epidermal growth factor receptor (EGFR) family signaling, is one of the major mechanisms contributing to Fulv resistance in patients with breast cancer (30, 31). As expected, exposure of MCF7 cells to Fulv for 10 d increased the levels of family members EGFR and HER2 (Fig. S5B). Treatment with low-dose ganetespib alone did not deplete total cellular levels of these kinases, as measured by immunoblot. Looking more closely at cell surface HER2 levels by flow cytometry, we did find a modest decline, suggesting that some impairment in the maturation of this very sensitive HSP90 client is caused by reducing HSP90 buffering capacity with low-dose ganetespib (Fig. S6). Most important, however, cotreatment with ganetespib and Fulv completely blocked the adaptive increase in EGFR and HER2 induced by Fulv (Fig. S5B). It also drove near-complete loss of phosphotyrosine signal in the SDS/PAGE migration position of all four EGFR family kinase members (175–185 kDa). Probing downstream of receptor signaling, we also found that similar to Tam (Fig. 2C), Fulv combination with ganetespib increased the depletion of diverse proteins associated with cell cycle progression and proliferation (Fig. S5C).

Combination Treatment Inhibits the Emergence of Resistance in Xenografts. Can low-level, noncytotoxic HSP90 inhibition limit the emergence of hormone resistance in vivo? To address this question, we used a xenograft model in which MCF-7 tumors were established in estrogen-supplemented mice. We defined a low-dose, twice-weekly schedule for the water-soluble ganetespib prodrug (STA-1474) that demonstrated no antitumor activity on its own (Fig. 4A). Tamoxifen was administered using a standard dose and schedule that slowed tumor progression, but consistent with previous reports (30), it failed to provide durable control in our model (Fig. 4A). However, when tamoxifen was combined with low-dose STA-1474, which had no effect on its own, we saw a marked, persistent improvement in tumor control.

This improvement in efficacy appeared to arise from a decline in the emergence of resistance to tamoxifen monotherapy. By day 39 of the experiment, considerable heterogeneity in tumor burden had developed in the tamoxifen-alone treatment group, but not the combination group (Fig. 4B). The marked ability of the combination treatment to reduce heterogeneity in treatment response translated into a dramatic improvement in event-free survival (Fig. 4C).

The different outcomes for these treatment regimens were reflected at the histologic level in tumors analyzed by H&E staining (Fig. 4D). Tumors from vehicle-treated mice showed relatively homogenous sheets of poorly differentiated adenocarcinoma sparingly infiltrated with stromal and connective tissue elements. The tumors of the STA-1474 group were similar. In contrast, tamoxifen-treated tumors showed small nests of tumor cells within dense bands of infiltrating fibrous stroma. Even more strikingly, combination-treated tumors showed extensive vacuolization in addition to the fibrotic changes seen in tamoxifen-treated tumors.

At the molecular level, the up-regulation of ER and HER2 levels induced by tamoxifen alone was blocked by combination treatment with tamoxifen and low-dose ganetespib (Fig. S7 A and B), consistent with effects seen in cell culture (Fig. S5 A and B). In addition, tumors exposed to the combination of tamoxifen and STA-1474 showed increased differentiation, as monitored by membranous expression of the epithelial marker MUC1, which is typically lost during malignant progression (32) (Fig. S8). In MCF-7 xenografts, we found only scant cytoplasmic staining in vehicle-treated animals. In contrast, MUC1 expression was strongly up-regulated in tumors treated with tamoxifen/STA-1474 and exhibited a membranous staining pattern reminiscent of normal breast tissue (Fig. 4E). Along with evidence of cyto-differentiation, combination treatment induced profound cell
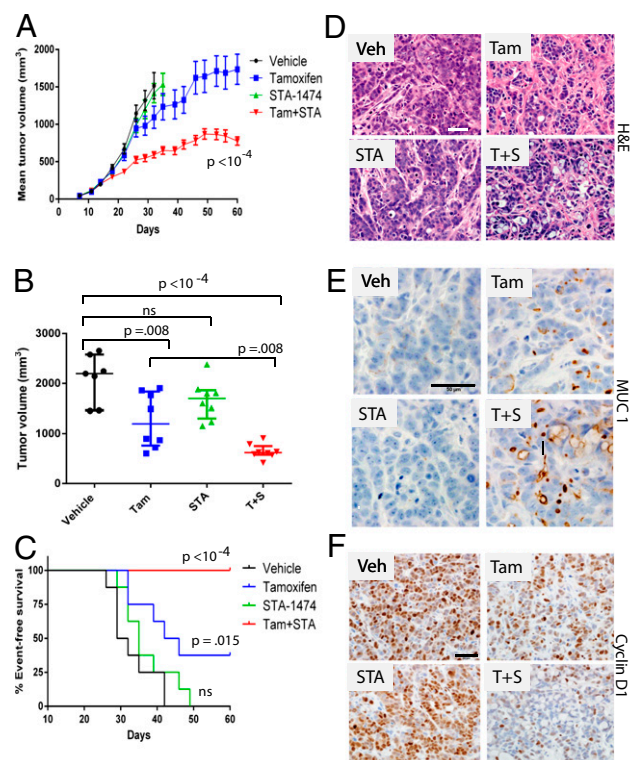

Fig. 4. Low-level HSP90 inhibition, having no effect on its own, limits the emergence of Tam resistance in mice and prolongs survival. (A) Antitumor activity of single-agent and combination treatments in estrogen-supplemented mice bearing MCF-7 xenografts. Mean tumor volume (eight mice per treatment group) is plotted. Bars, SEM. P value for the difference between Tamoxifen and Tam + STA groups was determined by two-way repeated-measures ANOVA. (B) Heterogeneity in tumor size within treatment groups at day 39 after cell implantation is reduced by combination treatment. Horizontal bars indicate median with interquartile range. P values were determined by Student t test (two-sided, unpaired). ns, not significant. (C) Combination treatment markedly prolongs event-free survival. Kaplan-Meier analysis is presented, using death or euthanasia for body condition score <2 or excess tumor volume (>1,500 mm^3) as event endpoints. The P values for differences from vehicle control were determined by Log-rank test. (D) H&E staining reveals a marked effect of combination treatment on tumor histology. Images were acquired at the same magnification. (Scale bar, 50 μm.) (E) Combination treatment increases expression of membranous MUC1 staining, as monitored by immunohistochemistry (IHC). (Scale bar, 50 μm.) (F) Combination treatment enhances depletion of Cyclin D1 levels detected by IHC. (Scale bar, 50 μm.)

cycle arrest in xenografts as well. The mitotic index of tumors was uniformly low across all samples in the combination treatment group (Fig. S7C). Cyclin D1 and phospho-retinoblastoma protein (RB) were also reduced to a much greater extent than was achieved by tamoxifen alone (Fig. 4E and Fig. S7D). As in cell culture, more profound and homogeneous cell cycle withdrawal was a hallmark of combination treatment.

Discussion

Previous studies across a wide spectrum of organisms have established the unique character of the HSP90 protein-folding buffer and how it facilitates the evolution of diverse new biological phenotypes, including drug resistance (1, 2, 5, 6, 9). Now we show that targeting this ancient, highly conserved role of HSP90 in supporting the evolution of new traits could provide a much needed approach to limiting the evolution of hormone resistance in ER+ breast cancer, a setting in which no curative treatment options exist for advanced disease.

Indeed, our data suggest that the current paradigm driving the clinical development of HSP90 inhibitors as broad-spectrum inhibitors of drug-resistant kinases is missing the greater clinical potential of these agents. Bolus dosing of current HSP90 inhibitors is well-tolerated and does transiently destabilize multiple oncogenic kinases, but systemic toxicity increases prohibitively as the duration of high-level HSP90 inhibition is extended. Unfortunately, HSP90 client levels return to baseline within a few days of drug administration, and high-level inhibition comes at the cost of stimulating tumor-supportive HSF1 activation. In contrast, we now report that very modest, sustained inhibition of HSP90, at well-tolerated levels that do not deplete clients on their own or activate HSF1, reduces heterogeneity in the response of tumors to antiestrogens and prolongs the duration of disease control by these agents. Focusing on these striking effects of low-level, noncytotoxic HSP90 inhibition, the current study provides a new perspective, one very different from the many previous reports describing interesting activity for high-level HSP90 inhibition against recurrent drug-resistant cancers (33–36) or synergistic interaction with other chemotherapeutics to increase their activity (37–39). From a translational perspective, the recent development of orally bioavailable HSP90 inhibitors should make sustained, low-level inhibitor exposure feasible in patients. The identification of genes that are modulated by ganetespib at lower concentrations than classical heat-shock protein genes suggests an approach to therapeutic monitoring in patients that targets dose levels that modulate these sensitive genes while sparing induction of heat-shock protein genes, the antithesis of current dosing strategies that have sought to maximize heat-shock induction as a pharmacodynamic endpoint.

Even at initial diagnosis, tremendous heterogeneity is seen in cellular levels of the ER protein, both within an individual breast tumor and between different tumors. Any level of ER expression (i.e., >1% of cells) is considered "ER positive," although patients with tumors demonstrating 1–10% staining appear to derive less benefit from endocrine therapy than those with 10% or higher staining. Such heterogeneity is also a feature of our MCF-7 xenograft model, in which cells within vehicle control tumors were seen with little or no ER staining, despite the majority being positive (Fig. S7A, Veh). For reasons that are not clear, however, hormonal therapy does not usually drive the outgrowth of ER-negative cells either in patients (22) or in our xenograft model (Fig. S7A, Tam and T+S). For the vast majority of patients with ER+ tumors, receptor expression is preserved and alternate, ligand-independent modes of activation involving oncogenic switching or constitutively activating mutation are seen. Often, heterogeneity in resistance mechanisms can be seen even within the tumor burden of a single patient, as dramatically illustrated by a recent study of ex vivo cultured circulating tumor cells isolated from patients with advanced ER+ breast cancer (40). Importantly, in this study, cells with clinically acquired resistance to multiple types of endocrine therapy demonstrated increased sensitivity to low-level HSP90 inhibition, suggested by the authors to be a result of the extreme dependence of their mutant ER on HSP90 for stability.

With so many avenues to resistance available, perhaps it is not surprising that clinical trials in patients with metastatic breast cancer combining endocrine therapy with inhibitors that selectively target individual bypass proteins have been disappointing (41, 42). So how is low-level HSP90 inhibition different? Our data show that it is not short-term pharmacological synergy. Rather, combination therapy limits tumor adaptation and escape from the cytostatic effects of disrupting ER function. As evidenced by such endpoints as CDK4 levels, RB phosphorylation, and E2F-regulated gene expression, a far more profound block to cell cycle progression is enforced by extended combinatorial treatment than can be achieved with either low-level HSP90 inhibition or hormone antagonists alone (27, 28). Viewed from an evolutionary perspective, this loss of replicative potential is likely to be a major factor in limiting the accumulation of de novo mutations or the emergence of preexisting resistant clones within a heterogeneous tumor cell population (20).

Intriguing clinical support for this hypothesis comes from a recent report describing significant clinical benefit on combining the cyclin-dependent kinase inhibitor PD-0332991 with an estrogen-depleting aromatase inhibitor (43). Because prolonged exposure to the combination of Fulv or tamoxifen with ganetespib is associated with the impairment of multiple bypass pathways, as well as impairment of ER function itself, the cell cycle block we demonstrate for combination of these antagonists with HSP90 inhibitor could provide even more durable disease control than a CDK + aromatase inhibitor combination.

Since the initial discovery of natural products that inhibit HSP90 over 2 decades ago, tremendous progress has been made in developing potent and specific drugs with which to target this chaperone. The most efficacious way to use these compounds in cancer therapy, however, remains to be defined. With their potential to act as inhibitors of the intrinsic ability of tumors to evolve, we now suggest they could provide a much-needed approach to controlling the emergence of drug resistance, which is perhaps the greatest current barrier to the development of curative therapies.

Materials and Methods

Cell Lines and Reagents. The human breast cancer cell lines MCF-7, T-47D, ZRF-75.1, and HCC-38 were obtained from the American Type Culture Collection, cultured under standard conditions, and confirmed to be negative for mycoplasma contamination by monthly surveillance testing. Sources for all chemical reagents and methods for their formulation are detailed in *SI Materials and Methods*.

Clonogenic Drug-Resistance Assays. Breast cancer cells were plated in 6-well format (10^5 cells per well) or 15-cm dish format (2×10^6 cells per dish) and allowed to adhere overnight. Compounds were added the following day, and cultures were refed with fresh drug-containing medium twice weekly for 4 wk. Wells were then fixed in cold methanol and stained with toluidine blue (0.1%) or Diff-Quik. To measure their relative cell content, fixed wells were incubated with the fluorescent DNA-binding dye Sytox Green (Invitrogen, 500 nM in PBS for 30 min) before Diff-Quik staining and relative fluorescence intensity was determined, using a multiwell plate reader (Safire²; Tecan).

Gene Knockdown and Flow Cytometry. Lentiviral pLKO.1-puro shRNA constructs were obtained from the Broad Institute RNAi platform. The specific sequence information is provided in *SI Materials and Methods*. Viral supernatants were prepared by standard methods and used to infect MCF-7 cells, followed by selection in puromycin (InvivoGen) for 10 d. Stably transduced cells were subcultured for 1 mo before measurement of HSP90 levels by immunoblotting, using antibodies directed against HSP90α (SPA-771), HSP90β (SPA-843), and total HSP90 (SPA-835, all HSP90 antibodies from StressGen/Enzo). Flow cytometric measurement of relative l HER-2 and IGF1 receptor levels on the surface of stably transduced MCF-7 cells was performed, using standard methods, as described in *SI Materials and Methods*.

Proliferation and Survival Assays. The measurement of relative viable cell numbers was performed in 96-well microplate format, using the fluorescent detection (Ex/Em: 540/590) of resazurin dye reduction as an endpoint. To measure cell mass independent of potential metabolic changes induced by drug exposure, plates were stained with 0.4% sulforhodamine B solution (In Vitro Toxicology Assay Kit; Sigma), per the manufacturer's instructions.

mRNA Expression Profiling and Analysis. MCF-7 cells were treated for 10 d, followed by RNA extraction, using an RNeasy kit per the manufacturer's recommendation (Qiagen). Genome-wide expression analysis was performed using Agilent 8 × 60K multiplex arrays. Data are provided in Dataset S1 and were processed as previously described (14). Gene set enrichment analysis of differentially expressed genes after drug treatment was performed using the Molecular Signatures Database (MsigDB) Web site, release version 3.84 (44).

E2F Reporter Assays. Breast cancer cells were stably transduced with a commercial lentiviral construct encoding firefly luciferase under control of a minimal CMV promoter and tandem repeats of an E2F-response element (Cignal Lenti E2F Reporter, SABiosciences). After puromycin selection, transduced cells were plated in 24-well format. Compounds were added the following day, and cultures were refed with fresh drug-containing medium every 3 d. After 9 d of treatment, wells were rinsed with PBS and cells were lysed in nondenaturing buffer. Lysates were assayed for luciferase activity using Steady-Glo reagent (Promega) and protein concentration, determined by bicinchoninic acid assay (BCA, Pierce/Thermo).

Immunohistochemical Staining. MCF-7 tumor xenografts were processed as formalin-fixed, paraffin-embedded tissue blocks. Antigen retrieval was performed on deparaffinized sections, using a pressure cooker with Dako citrate buffer (pH 6.0) at $122 \pm 2\ °C$, 15 ± 5 psi for 45 s. Sections were then incubated with primary antibodies (see *SI Materials and Methods* for details). Detection was achieved by incubation for 30 min at room temp with polymer anti-rabbit-HRP (DakoCytomation) and signal developed in 3,3'-Diaminobenzidene for 3 min, followed by counterstaining with Gill hematoxylin.

Immunoblotting. Whole-cell protein extracts were prepared in nondenaturing lysis buffer and immunoblotted to measure the relative levels of specific proteins, using standard methods, as detailed in *SI Materials and Methods*.

Xenograft Tumor Model. Female nonobese diabetic-SCID mice were estrogen-supplemented by s.c. implantation of slow-release 17β-estradiol pellets (0.72 mg/90-d release; Innovative Research of America) 1 d before MCF-7 tumor cell injection into the mammary fat pad (5×10^6 MCF-7 cells suspended in a 1:1 PBS:Matrigel solution). Details for the measurement of tumor volume and treatment protocol with tamoxifen citrate and HSP90 inhibitor are provided in *SI Materials and Methods*. Treatments were continued for the entire duration of the experiment. All mouse experiments were performed under protocols approved by Institutional Committees on Animal Care at either the Massachusetts Institute of Technology or Synta Pharmaceuticals.

Statistical Methods. All statistical analyses were performed using Prism 6.0 (GraphPad software). Statistical significance cutoff for all comparisons was $P < 0.05$.

1. Jarosz DF, Lindquist S (2010) Hsp90 and environmental stress transform the adaptive value of natural genetic variation. *Science* 330(6012):1820–1824.
2. Rohner N, et al. (2013) Cryptic variation in morphological evolution: HSP90 as a capacitor for loss of eyes in cavefish. *Science* 342(6164):1372–1375.
3. Taipale M, et al. (2012) Quantitative analysis of HSP90-client interactions reveals principles of substrate recognition. *Cell* 150(5):987–1001.
4. Samant RS, Clarke PA, Workman P (2012) The expanding proteome of the molecular chaperone HSP90. *Cell Cycle* 11(7):1301–1308.
5. Queitsch C, Sangster TA, Lindquist S (2002) Hsp90 as a capacitor of phenotypic variation. *Nature* 417(6889):618–624.
6. Rutherford SL, Lindquist S (1998) Hsp90 as a capacitor for morphological evolution. *Nature* 396(6709):336–342.
7. Cetinbaş M, Shakhnovich EI (2013) Catalysis of protein folding by chaperones accelerates evolutionary dynamics in adapting cell populations. *PLOS Comput Biol* 9(11): e1003269.
8. Cowen LE, et al. (2009) Harnessing Hsp90 function as a powerful, broadly effective therapeutic strategy for fungal infectious disease. *Proc Natl Acad Sci USA* 106(8): 2818–2823.
9. Vincent BM, Lancaster AK, Scherz-Shouval R, Whitesell L, Lindquist S (2013) Fitness trade-offs restrict the evolution of resistance to amphotericin B. *PLoS Biol* 11(10):e1001692.
10. Whitesell L, Mimnaugh EG, De Costa B, Myers CE, Neckers LM (1994) Inhibition of heat shock protein HSP90-pp60v-src heteroprotein complex formation by benzoquinone ansamycins: Essential role for stress proteins in oncogenic transformation. *Proc Natl Acad Sci USA* 91(18):8324–8328.
11. Xu Y, Lindquist S (1993) Heat-shock protein hsp90 governs the activity of pp60v-src kinase. *Proc Natl Acad Sci USA* 90(15):7074–7078.
12. Trepel J, Mollapour M, Giaccone G, Neckers L (2010) Targeting the dynamic HSP90 complex in cancer. *Nat Rev Cancer* 10(8):537–549.
13. Whitesell L, Lindquist SL (2005) HSP90 and the chaperoning of cancer. *Nat Rev Cancer* 5(10):761–772.
14. Mendillo ML, et al. (2012) HSF1 drives a transcriptional program distinct from heat shock to support highly malignant human cancers. *Cell* 150(3):549–562.
15. Scherz-Shouval R, et al. (2014) The reprogramming of tumor stroma by HSF1 is a potent enabler of malignancy. *Cell* 158(3):564–578.
16. Acquaviva J, et al. (2014) mTOR inhibition potentiates HSP90 inhibitor activity via cessation of HSP synthesis. *Mol Cancer Res* 12(5):703–713.
17. Powers MV, Clarke PA, Workman P (2008) Dual targeting of HSC70 and HSP72 inhibits HSP90 function and induces tumor-specific apoptosis. *Cancer Cell* 14(3):250–262.
18. Lin NU, Winer EP (2008) Optimizing endocrine therapy for estrogen receptor-positive breast cancer: Treating the right patients for the right length of time. *J Clin Oncol* 26(12):1919–1921.
19. Oesterreich S, Davidson NE (2013) The search for ESR1 mutations in breast cancer. *Nat Genet* 45(12):1415–1416.
20. Bozic I, et al. (2013) Evolutionary dynamics of cancer in response to targeted combination therapy. *eLife* 2:e00747.
21. Rosenberg SM, Queitsch C (2014) Medicine. Combating evolution to fight disease. *Science* 343(6175):1088–1089.
22. Polyak K (2014) Tumor heterogeneity confounds and illuminates: A case for Darwinian tumor evolution. *Nat Med* 20(4):344–346.
23. Nugoli M, et al. (2003) Genetic variability in MCF-7 sublines: Evidence of rapid genomic and RNA expression profile modifications. *BMC Cancer* 3:13.
24. Friedland JC, et al. (2014) Targeted inhibition of Hsp90 by ganetespib is effective across a broad spectrum of breast cancer subtypes. *Invest New Drugs* 32(1):14–24.

25. Ying W, et al. (2012) Ganetespib, a unique triazolone-containing Hsp90 inhibitor, exhibits potent antitumor activity and a superior safety profile for cancer therapy. *Mol Cancer Ther* 11(2):475–484.
26. Nijman SM, Friend SH (2013) Cancer. Potential of the synthetic lethality principle. *Science* 342(6160):809–811.
27. Miller TW, et al. (2011) ERα-dependent E2F transcription can mediate resistance to estrogen deprivation in human breast cancer. *Cancer Discov* 1(4):338–351.
28. Stender JD, et al. (2007) Estrogen-regulated gene networks in human breast cancer cells: Involvement of E2F1 in the regulation of cell proliferation. *Mol Endocrinol* 21(9):2112–2123.
29. Beliakoff J, et al. (2003) Hormone-refractory breast cancer remains sensitive to the antitumor activity of heat shock protein 90 inhibitors. *Clin Cancer Res* 9(13):4961–4971.
30. Massarweh S, et al. (2008) Tamoxifen resistance in breast tumors is driven by growth factor receptor signaling with repression of classic estrogen receptor genomic function. *Cancer Res* 68(3):826–833.
31. Osborne CK, et al. (2011) Gefitinib or placebo in combination with tamoxifen in patients with hormone receptor-positive metastatic breast cancer: A randomized phase II study. *Clin Cancer Res* 17(5):1147–1159.
32. Rakha EA, et al. (2005) Expression of mucins (MUC1, MUC2, MUC3, MUC4, MUC5AC and MUC6) and their prognostic significance in human breast cancer. *Mod Pathol* 18(10):1295–1304.
33. Acquaviva J, et al. (2014) Overcoming acquired BRAF inhibitor resistance in melanoma via targeted inhibition of Hsp90 with ganetespib. *Mol Cancer Ther* 13(2):353–363.
34. Bachleitner-Hofmann T, et al. (2011) Antitumor activity of SNX-2112, a synthetic heat shock protein-90 inhibitor, in MET-amplified tumor cells with or without resistance to selective MET Inhibition. *Clin Cancer Res* 17(1):122–133.
35. Sang J, et al. (2013) Targeted inhibition of the molecular chaperone Hsp90 overcomes ALK inhibitor resistance in non-small cell lung cancer. *Cancer Discov* 3(4):430–443.
36. Wong C, Wang X, Smith D, Reddy K, Chen S (2012) AKT-aro and HER2-aro, models for de novo resistance to aromatase inhibitors; molecular characterization and inhibitor response studies. *Breast Cancer Res Treat* 134(2):671–681.
37. De Raedt T, et al. (2011) Exploiting cancer cell vulnerabilities to develop a combination therapy for ras-driven tumors. *Cancer Cell* 20(3):400–413.
38. Miyajima N, et al. (2013) The HSP90 inhibitor ganetespib synergizes with the MET kinase inhibitor crizotinib in both crizotinib-sensitive and -resistant MET-driven tumor models. *Cancer Res* 73(23):7022–7033.
39. He S, et al. (2014) The HSP90 inhibitor ganetespib has chemosensitizer and radio-sensitizer activity in colorectal cancer. *Invest New Drugs* 32(4):577–586.
40. Yu M, et al. (2014) Cancer therapy. Ex vivo culture of circulating breast tumor cells for individualized testing of drug susceptibility. *Science* 345(6193):216–220.
41. Creighton CJ, et al. (2008) Development of resistance to targeted therapies transforms the clinically associated molecular profile subtype of breast tumor xenografts. *Cancer Res* 68(18):7493–7501.
42. Roop RP, Ma CX (2012) Endocrine resistance in breast cancer: Molecular pathways and rational development of targeted therapies. *Future Oncol* 8(3):273–292.
43. Finn RS, et al. (2012) Preliminary results of a randomized phase 2 study of PD 0332991, a cyclin-dependent kinase 4/6 inhibitor, in combination with letrozole for first-line treatment of patients with postmenopausal, ER-positive, HER2-Negative advanced breast cancer. San Antonio Breast Cancer Symposium (SABCS) (San Antonio), pp S1–S6. Available at www.cccnevada.com/wp-content/uploads/Finn_SABCS_Poster.pdf. Accessed November 24, 2014.
44. Subramanian A, et al. (2005) Gene set enrichment analysis: A knowledge-based approach for interpreting genome-wide expression profiles. *Proc Natl Acad Sci USA* 102(43):15545–15550.

Supporting Information

Whitesell et al. 10.1073/pnas.1421323111

SI Materials and Methods

Chemicals and Reagents. Geldanamycin, 4-hydroxytamoxifen, peanut oil, and Diff-Quick staining reagents were purchased from Sigma. Tamoxifen citrate was from Enzo/Alexis Biochemicals, and Fulv was obtained from Ontario Chemicals Inc. Ganetespib and its phosphate ester prodrug STA-1474 were provided by Synta Pharmaceuticals. For cell culture experiments, hormone antagonists were formulated in ethanol, whereas HSP90 inhibitors were formulated in DMSO. Stock solutions were made fresh monthly and maintained at −20 °C in the dark until use.

shRNA Sequences.

HSP90α (NM 005348)

α-1 (start position 616)	5′-GTTATCCTACACCTGAAAGAA-3′
α-2 (start position 867)	5′-GAAGGATGGTGACAAGAAGAA-3′

HSP90β (NM_007355)

β-1 (start position 2402)	5′-GCAGTAAACTAAGGGTGTCAA-3′
β-2 (start position 232)	5′-GCCTTGGACAAGATTCGCTAT-3′

Ctrl (EGFP-targeted sequence)	5′-GCAAGCTGACCCTGAAGTTCA-3′

Flow Cytometry. MCF-7 cells were harvested using Accumax (Innovative cell Technologies) and were incubated for 60 min on ice with primary mouse monoclonal antibodies [IGF1R: clone α-IR3 (EMD/Calbiochem) or phycoerythrin (PE)-conjugated HER2 (BD Biosciences 340879)]. After washing, cells stained with α-IR3 were subsequently incubated with Alexa-488 goat anti-mouse secondary antibody for 30 min on ice. After a final wash, cells (5,000–10,000 events per treatment condition) were analyzed using a Personal Cell Analyst (Guava/Millipore).

Immunohistochemistry. Formalin-fixed, paraffin-embedded tissue sections were probed with antibodies to the following proteins: Cyclin D1 (Cell Signaling no. 2978, clone 92G2, 1:50 dilution overnight), Phospho-RB (Cell Signaling no. 8516, clone D20B12, 1:200 dilution overnight), MUC-1 (Sigma no. HPA008855, 1:50 dilution for 1 h), ER (Neomarkers no. RM9101-S, clone SP1, 1:40 dilution for 1 h), and Phospho-p44/42 mitogen-activated protein kinase (Cell Signaling no. 4370, clone D13.14.4E, 1:500 dilution overnight).

Immunoblotting. Cell monolayers were lysed in cold buffer consisting of 100 mM NaCl, 30 mM Tris·HCl at pH 7.6, 1% Nonidet P-40, 30 mM sodium fluoride, 1 mM EDTA, 1 mM sodium vanadate, and complete protease inhibitor mixture tablet (Roche Diagnostics). Samples were incubated on ice for 30 min, and postnuclear supernatants were recovered by centrifugation at 14,000 rpm at 4 °C for 10 min. Protein concentrations were determined using BCA (Pierce Biochemical). Proteins were separated on NuPAGE Novex gels and transferred to nitrocellulose membranes. Membranes were blocked with 3% (wt/vol) nonfat dry milk in PBS (pH 7.4) and washed with PBS (pH 7.4) containing 0.05% Tween-20. Membranes were probed with antibodies against the following proteins: CDK4 (pAb C-22; Santa Cruz Biotechnology), Cyclin D1 (Clone DCS-6; EMD Millipore/Calbiochem), c-MYC (Clone 9E10; Santa Cruz), alpha-tubulin (Clone B-5–1-2; Sigma), ER (Ab 17, mixture of clones 1D5 and 6F11; Neomarkers/Thermo), β-actin (catalog no. 970; Cell Signaling Technology), HER2 (AB17, mixture of clones E2-4001 and 3B5; Neomarkers/Thermo), EGFR (catalog no. 4267; Cell Signaling), IGF1R (catalog no. 556000; BD Biosciences), phosphotyrosine (Clone 4G10; Millipore), p70S6K (catalog no. 2708; Cell Signaling), and S6 kinase (catalog no. 9202; Cell Signaling). Detection was achieved by incubation with peroxidase-conjugated, species-appropriate secondary antibodies, followed by chemiluminescent detection.

Xenograft Tumor Model. When MCF-7 tumor xenografts reached a mean volume of ~200 mm^3 (length × width^2/2), mice were randomly assigned to experimental treatment groups (eight mice/group). Tamoxifen citrate was administered s.c. as an emulsion in peanut oil (0.5 mg/mouse) daily, 5 d per week. The ganetespib prodrug STA-1474 was administered intraperitoneally on a dose and schedule (25 mg/kg, equivalent to 21 mg/kg ganetespib, on 2 consecutive days per week) determined by pilot experiments to exert no effect on tumor progression as a single agent. This dose is less than 20% the recommended minimally toxic single-agent dose (125 mg/kg) for ganetespib used on a once-weekly schedule for most preclinical mouse studies performed by its manufacturer.

Fig. S1. Modest pharmacological inhibition of HSP90 function by different compound classes limits the emergence of Tam resistance in cell culture. (*A*) MCF-7 cells were cultured continuously in the presence of the indicated concentrations of the HSP90 inhibitor, ganetespib (Gan), with or without concurrent Tam (1 μM). After 1 mo, cells were fixed with cold methanol and visualized by staining with Diff-Quik. Photomicrographs of representative fields are provided at identical magnification in all panels. (*B*) MCF-7 cells were cultured continuously in the presence of the HSP90 inhibitor, geldanamycin (20 nM), with or without concurrent Tam (5 μM). After 1 mo, cells were fixed with cold methanol and visualized by staining with toluidine blue. Macroscopic images of representative fields are provided at the same scale in all panels.
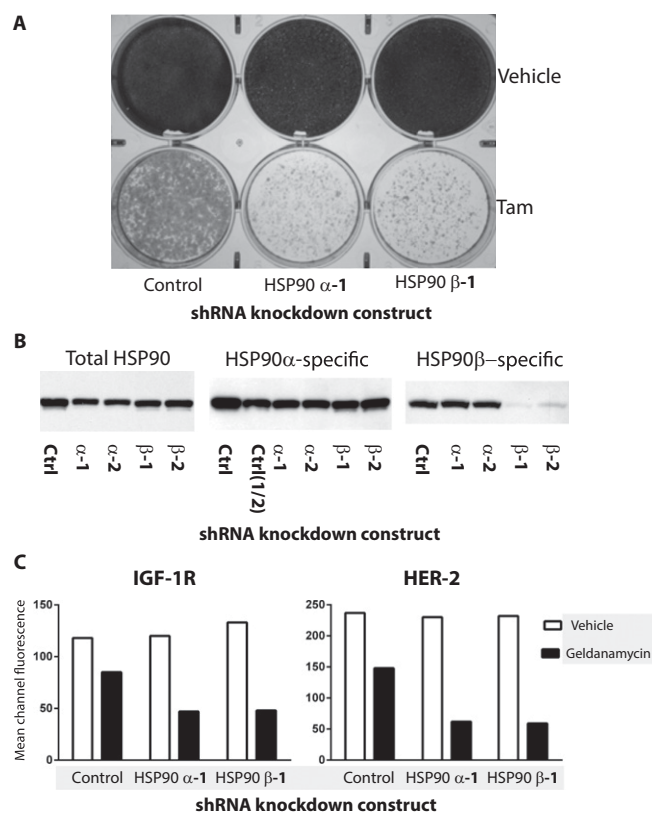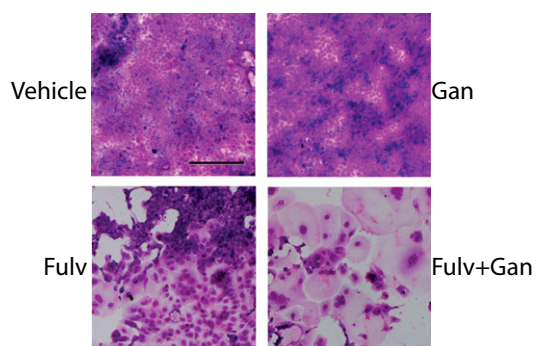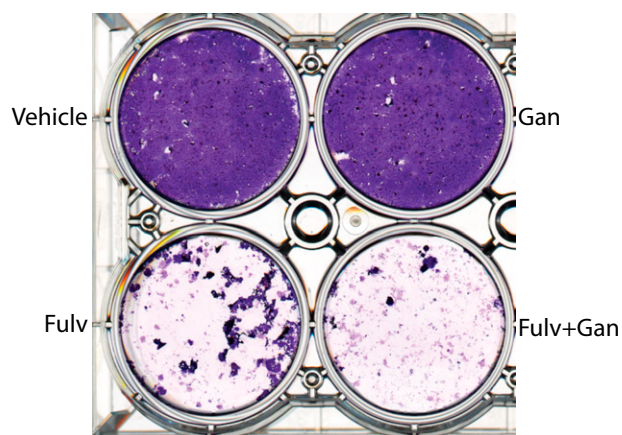
Fig. S2. Modest genetic knockdown of HSP90 limits the emergence of tamoxifen resistance in cell culture and sensitizes cells to the effects of an HSP90 inhibitor. (*A*) Clonogenic resistance assay: MCF-7 cells were stably transduced with lentiviral constructs encoding shRNA targeting HSP90α, HSP90β, or an irrelevant control construct. Cells were cultured for 1 mo in the continuous presence of 4-hydroxytamoxifen (Tam, 1 μM) or an equal volume of solvent vehicle (ethanol, 0.01% vol/vol), fixed with cold methanol, and stained with toluidine blue to visualize the outgrowth of resistant colonies. (*B*) Immunoblotting with the indicated anti-HSP90 antibodies was used to assess relative HSP90 isoform levels in MCF-7 cells after stable transduction with two independent lentiviral shRNA constructs targeting each HSP90 isoform. Ctrl, shRNA construct targeting EGFP; Ctrl (1/2), a lane in which half the amount of control lysate total protein was loaded. (*C*) Immunostaining of live cells followed by flow cytometry for the indicated HSP90 client receptors was performed to measure the effect of modest HSP90 knockdown on cell-surface levels in the absence (vehicle) or presence of the HSP90 inhibitor geldanamycin (1 μM, overnight exposure).

Fig. S3. Mining of genome-wide transcriptional profiling data (Dataset S1) demonstrates that low-concentration ganetespib alone (10 nM for 10 d) does not induce the expression of classical heat-shock-protein genes (*A*) or consistently down-regulate the expression of estrogen-responsive genes (*B*).

ZRF-75.1
ER+ Breast Cancer

Scale bar
100 μm

Fig. S4. Low-concentration ganetespib (Gan; 10 nM) has no effect on its own but causes a marked reduction in the emergence of resistance to Fulv (1 μM) in the ER+ human breast cancer cell line ZRF 75.1. (*Upper*) Macroscopic images of Diff-Quick-stained wells after culture for 1 mo in the presence of the indicated compounds. (*Lower*) Photomicrographs obtained from the same wells. All micrographs were acquired at the same magnification. (Scale bar, 100 μm.)
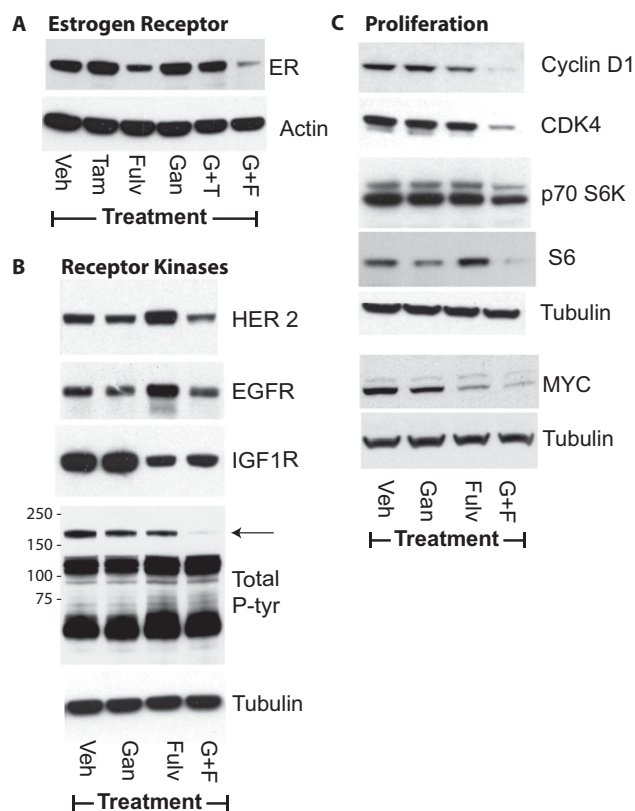
Fig. S5. Enhanced depletion of multiple signaling and growth-regulatory proteins in cells exposed to combination Fulv + ganetespib (Gan) treatment. Immunoblotting for the relative level of the indicated targets was performed on lysates prepared from MCF-7 cells exposed to the indicated compounds for 10 d at the following concentrations: Vehicle (DMSO 0.1% + ethanol 0.01%), Tam (1 μM), Fulv (1 μM), Gan (10 nM), G+T and G+F (10 nM + 1 μM). (*A*) Estrogen receptor levels are reduced more by combination treatments than by single agents. (*B*) EGFR-family tyrosine kinase protein levels tyrosine phosphorylation are reduced by Gan+ Fulv combination treatment more than by either agent alone. (*C*) Depletion of diverse proliferation-associated proteins is increased by combination drug exposure. Actin or tubulin is blotted as a loading control in each panel.
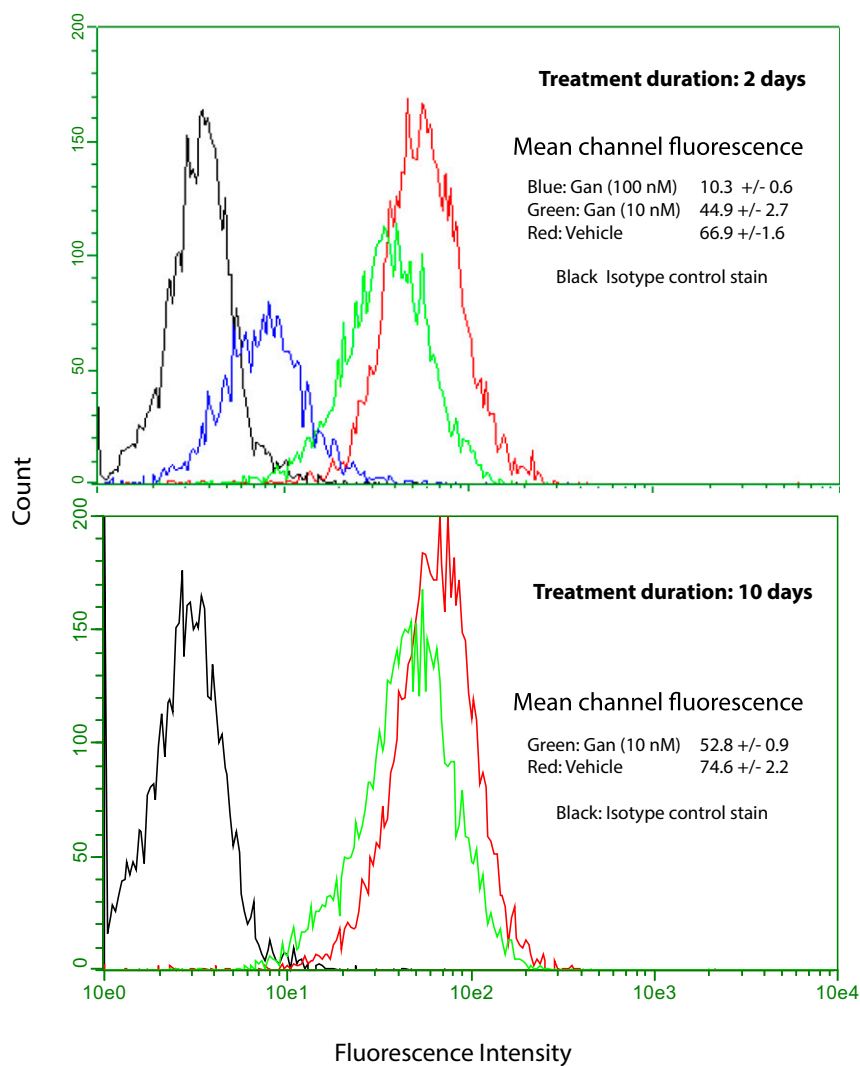
Fig. S6. Compromise of HSP90 chaperone capacity by low-dose ganetespib mildly impairs maturation of the client receptor kinase HER2. (*A*) MCF-7 cells were treated with the indicated concentrations of ganetespib (Gan) for 2 d before the immunostaining of live cells for HER2 and the determination of relative cell surface levels (mean channel fluorescence) by flow cytometry. The mean of three independent biological replicates ± SD is indicated for each treatment condition. An overlay plot of a single representative histogram for each treatment is also presented. (*B*) MCF-7 cells were treated for 10 d and then immunostained and analyzed as described for *A*.

Fig. S7. Combination treatment of xenograft-bearing mice enhances cell cycle withdrawal and limits adaptive responses to tamoxifen. (*A*) Combination treatment with STA-1474 and tamoxifen blocks tamoxifen-induced up-regulation of ER levels in tumor xenografts, as measured by IHC. (*B*) Combination treatment blocks tamoxifen-induced up-regulation of HER2 levels in tumor xenografts, as measured by IHC. (*C*) Mitotic index for tumors in each treatment group was determined by visual examination of 10 high-powered fields, using H&E-stained sections. Horizontal bars depict the median with interquartile range for each treatment group. *P* values were determined by Student *t* test (two-sided, unpaired). NS, not significant. (*D*) Combination treatment enhances depletion of phospho-RB levels detectable in tumor xenografts by IHC. Representative photomicrographs are presented at identical magnification. (Scale bar, 50 μm.)

Fig. S8. Immunostaining of human breast samples for MUC1 demonstrates loss of membranous expression during malignant transformation and progression. DCIS, ductal carcinoma in situ; grade I and II, invasive ductal carcinoma.

Other Supporting Information Files

Dataset S1 (XLSX)